Journal of Clinical & Experimental Ophthalmology

Cesareo et al., J Clin Exp Ophthalmol 2016, 7:2
http://dx.doi.org/10.4172/2155-9570.1000538

Research Article Open Access

Automatic Segmentation of Posterior Pole Retinal Layers In Patients with Early Stage Glaucoma Using Spectral Domain Optical Coherence Tomography

Massimo Cesareo[1*], **Elena Ciuffoletti**, **Alessio Martucci**, **Carlo Balducci**, **Andrea Cusumano**, **Federico Ricci and Roberto Pietro Sorge**[2]

[1]*Ophthalmology Unit, Department of Experimental Medicine and Surgery, University of Rome "Tor Vergata", Rome, Italy*

[2]*Laboratory of Biometry, Department of Systems Medicine, University of Rome "Tor Vergata", Rome, Italy*

[*]**Corresponding author:** Massimo Cesareo MD, PhD, Ophthalmology Unit, Department of Experimental Medicine and Surgery, University of Rome Tor Vergata, Via Montpellier , 00133 Rome, Italy, Tel: +390620903573; Fax: +39062026232; E-mail: massimo.cesareo@uniroma2.it

Received date: January 08, 2016; **Accepted date:** April 01, 2016; **Published date:** April 05, 2016

Copyright: © 2016 Cesareo M, et al. This is an open-access article distributed under the terms of the Creative Commons Attribution License, which permits unrestricted use, distribution, and reproduction in any medium, provided the original author and source are credited.

Abstract

Purpose: To measure Ganglion Cell Layer (GCL) and Retinal Nerve Fiber Layer (RNFL) thickness of the retinal posterior pole in patients with early stage primary open-angle glaucoma (POAG) using the new automatic segmentation technology of spectral domain optical coherence tomograph (SD-OCT).

Methods: 37 clinical records of patients with early glaucoma (grade 1 to 2 according to the Glaucoma Staging System 2) and 40 age and sex-matched controls were considered in this case-control observational retrospective study. Automated segmentation of GCL and RNFL was performed in one randomly selected eye from the electronic OCT records of each participant using the new Spectralis SD-OCT segmentation technology (Heidelberg Engineering, Inc., Heidelberg, Germany). Thickness of different retinal layers was obtained from each Posterior Pole volumetric scan. Measurements of the peripapillary RNFL thickness (pRNFLt) were also obtained and then compared with those of posterior pole RNFL thickness (ppRNFLt).

Results: Both GCL and RNFL were significantly thinner at the retinal posterior pole in the POAG group as compared to the control group (p<0,0001). Furthermore, pRNFLt was significantly thinner in the glaucoma group as opposed to the control group (p<0,0001). Measurements of pRNFLt were significantly correlated with those of the ppRNFLt (Pearson's coefficient r=0.863).

Conclusions: The new Spectralis SD-OCT automatic segmentation tool may be useful in evaluating structural damage in patients with early glaucoma, by providing complementary measurements to the clinical assessment of glaucoma that could be used in conjunction with other relevant parameters in the diagnosis and the evaluation of the progression of the disease.

Keywords: Glaucoma; SD-OCT; Ganglion cell layer; Retinal nerve fiber layer; Retinal posterior pole

Introduction

Glaucoma is an optic neuropathy that can lead to progressive and irreversible vision loss due to ganglion cell death. It clinically manifests as characteristic optic nerve head (ONH) and retinal nerve fiber layer (RNFL) alterations with correlating visual field changes [1] and represents the second cause of partially preventable blindness globally [2]. Optical coherence tomography, a well-accepted tool for the assessment of glaucomatous structural alterations, enables objective measurement of peripapillary RNFL and macular thickness [3-7]. Thinning of the retinal nerve fiber layer (RNFL) and of the ganglion cell complex (GCC) occurs as glaucoma progresses [8].

Spectral-Domain Optical Coherence Tomography (SD-OCT) is a more recent technique that allows the imaging of ocular structures with higher resolution and faster scan rates compared with the previous version of this technology (Stratus OCT, Carl Zeiss Meditec Inc., Dublin, CA, USA) [9,10].

Retinal 3D OCT volumes are now commonly acquired for clinical diagnosis or investigation. The accurate and rapid quantification of large volumes of data is of great value for clinicians and scientists to quickly investigate retinal and optic nerve head alterations.

Evaluation of intra-retinal layer thickness plays an important role in the diagnosis and monitoring of various ocular diseases.

Several computer-automated algorithms for intra-retinal layer segmentation have been proposed to overcome the limits of most of the commercial systems, in terms of capacity to measure the thickness of only a few retinal layers. These algorithms applied to the high resolution SD-OCT instruments allow quantitative evaluation of the thickness of all intra-retinal layers [11].

Segmentation is a critical step towards reliable quantification of total retinal, RNFL and GCC thickness that actually represent helpful parameters in elucidating either the presence or progression of glaucoma. However, fully automated segmentation of retinal OCT scans is challenging due to intrinsic speckle noise, the possible presence of blood vessels and other artifacts (e.g. motion, reduced illumination).

The aim of this case-control study was to evaluate the Ganglion Cell Layer (GCL) and Retinal Nerve Fiber Layer (RNFL) thickness at the retinal Posterior Pole in patients with early stage primary open angle glaucoma (POAG) and to compare the obtained results with those of

healthy subjects, using the new "Spectralis" spectral domain optical coherence tomography (SD-OCT) segmentation technology (Spectralis device, software version 6.0).

Materials and Methods

The study was approved by the internal review board of the University Hospital of Tor Vergata, Rome and the research followed the tenets of the Declaration of Helsinki.

The medical records of 37 glaucoma patients from the glaucoma clinic of the University Hospital of Tor Vergata were included in this study.

All subjects considered in this study had extensive ophthalmologic examinations available in their clinical records, including best-corrected visual acuity (BCVA), Goldmann applanation tonometry, central corneal thickness (CCT) by ultrasound pachymetry measurements, gonioscopy, slit-lamp biomicroscopy with dilated fundus examination, Standard Automated Perimetry (SAP) with SITA-Standard program 24-2 of a Humphrey Field Analyzer (model 750, Zeiss Humphrey Systems, Dublin, CA, USA).

Diagnosis of glaucoma was based on the occurrence of typical glaucomatous optic disc changes with corresponding visual field defects. Optic disc changes consisted in cup-to-disc ratio (CDR) greater than 0.5 in either eye and/or CDR asymmetry greater than or equal to 0.2 and/or presence of focal thinning of the rim in either eye.

A glaucomatous visual field defect was defined as a glaucoma hemifield test outside of the range of normal limits, pattern standard deviation (PSD) with a P value less than 5%, or a cluster of three points or more in the pattern deviation plot in a single hemifield (superior or inferior) with a P value of less than 5%, one of which having a P value of less than 1%.

All of the patients were classified as having early stage glaucoma (1 and 2) according to the Glaucoma Staging System 2 criteria [12].

All patients affected by glaucoma were treated in accordance with the EGS guidelines [13].

Those with the presence of any retinal pathology or optic nerve disease other than glaucoma and spherical or cylindrical refractive errors higher than 3 and 2 diopters (D) respectively identified in medical records were excluded.

Medical records of 40 age and sex-matched healthy subjects formed the control group. Inclusion criteria were as follows: spherical or cylindrical refractive errors lower than 3 and 2 D, respectively; normal intraocular pressure (<21 mmHg); normal CCT, normal appearance of the optic disc; normal visual field; no significant ocular disease found by routine ophthalmologic examination; and no family history of glaucoma or systemic diseases with possible ocular involvement.

Measurements of Posterior Pole RNFL and GCL thickness and peripapillary RNFL thickness were performed using SD-OCT imaging (Spectralis; Heidelberg Engineering, Heidelberg, Germany).

Both eyes of each included patient were considered, but only one eye was randomly chosen for statistical analysis.

Images were acquired using image alignment eye-tracking software (TruTrack; Heidelberg Engineering GmbH) as this improves scan reproducibility [14].

The Spectralis "Posterior Pole" scanning protocol (scanning area: 30° × 25°), comprising 61 single axial scans centered on the fovea with a fovea-to-disc inclination of 7 degrees, was used to obtain volumetric retinal scans.

"Posterior Pole" measurements from each SD-OCT scan were performed using the inbuilt Spectralis mapping software, the Heidelberg Eye Explorer (version 6.0c). The new Spectralis segmentation software was used to obtain the following thickness measurements: total retinal thickness (Retina), retinal nerve fiber layer (RNFL); ganglion cell layer (GCL); inner plexiform layer (IPL); inner nuclear layer (INL); outer plexiform layer (OPL); outer nuclear layer (ONL); retinal pigment epithelium (RPE). Moreover, the Automatic Segmentation tool of the Posterior Pole scan also provides thickness values of inner retinal layers (IRL) and outer retinal layers (ORL).

The Spectralis Posterior Pole total retinal thickness map (Retina) of a healthy subject is shown in Figure 1.

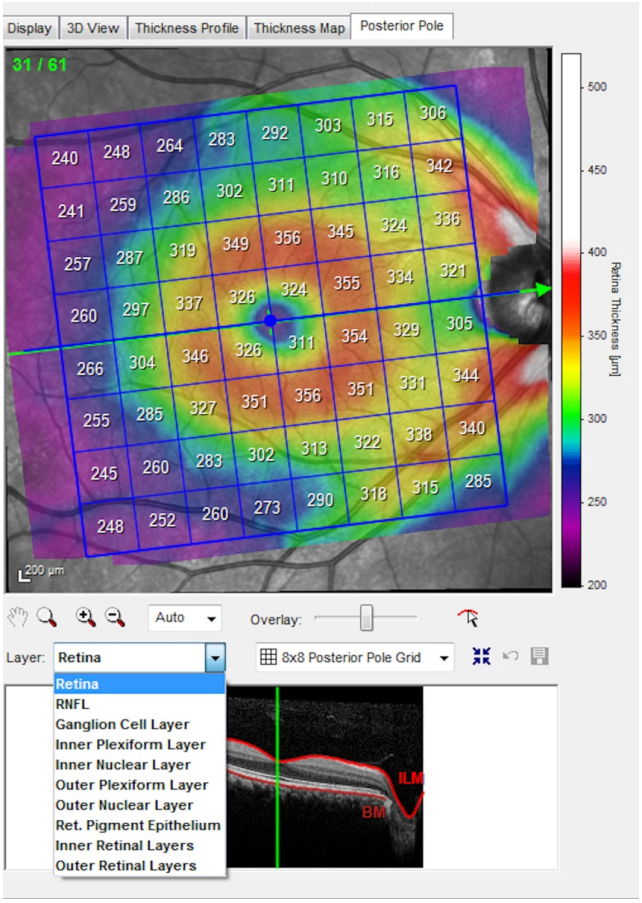

Figure 1: "Posterior Pole" overall retinal thickness map (Retina); in the lower-left corner the different retinal layers segmentation provided by the Spectralis SD-OCT are listed.

In addition, measurements of the peripapillary RNFL thickness (pRNFLt) using the RNFL-N Axonal Analytics protocol of the Spectralis OCT device were performed in all subjects. RNFL thickness was measured around the disc with 16 averaged, consecutive circular B-scans (diameter of 3.5 mm, 768 A-scans). pRNFLt represents the mean distance between the ILM and the posterior boundary of the

retinal nerve fiber layer, along a 6° radius circle scan centered on the optic nerve head.

All scans using the Posterior Pole and RNFLt protocols were acquired after pupil dilation with 0.5% tropicamide and 10% phenylephrine (Visumidriatic Fenilefrina, Visufarma).

Only high-quality scans, defined as scans with signal quality >25, where the quality score range is 0 (poor quality) to 40 (excellent quality), without discontinuity or misalignment, poor illumination, involuntary saccadic eye movements or blinking artifacts on careful visual inspection were used for analysis. The same experienced operator applied manual correction to the OCT automatic segmentation when necessary; however these cases were excluded from the study.

For maximum reproducibility, an internal fixation target was used [15]. In particular, to acquire the posterior pole and the peripapillary RNFL scans, the patient was asked to fixate on a central target and a nasal target, respectively.

Repeatability and reproducibility of the retinal layers thickness measurements obtained from the Spectralis posterior pole scans using the new segmentation algorithm were evaluated from the OCT electronical records of 8 healthy subjects who had undergone the Posterior Pole scan three times on the same day in the same eye. In particular, repeatability and reproducibility were calculated for each of the 64 volumetric units constituting the "posterior pole" scan map of each segmented layer.

Statistical analysis

All data were initially entered into an EXCEL database (Microsoft, Redmond, Washington – United States) and the analysis was performed using the SPSS vers. 20.0 (SPSS, Chicago, Illinois, USA) and the NCSS and PASS vers.11.0 for power analysis.

Values in the text and tables are presented as the mean ± standard deviation (SD). Preliminary analyses were performed to ensure that there was no violation of the assumptions of normality and linearity.

Descriptive statistics consisted of the mean ± standard deviation values for parameters with Gaussian distributions (after confirmation with histograms and the Kolgomorov-Smirnov test). The level of statistical power to detect a difference between the two groups was 99% with an alpha=0.5 for N=37 subjects.

The data were analyzed using a one-way analysis of variance (ANOVA) and a Bonferroni test for multiple comparisons.

The coefficient of variation (CV %) was used to determine repeatability and reproducibility of SD-OCT measurements of all the analyzed retinal layers, for each of the 64 volumetric units constituting the "posterior pole" scan map.

Pearson's test was used to identify statistical correlations between pRNFLt and ppRNFLt. A p value of <0.05 was considered statistically significant.

Results

A total of 37 eyes from 37 patients (22 males and 15 females, mean age 59.4 ± 7.6 years, range 49 to 70 years) with early stage glaucoma (18 stage 1 and 19 stage 2 POAG patients) and 40 eyes of 40 healthy individuals (23 males and 17 females, mean age 58.3 ± 9.7 years, range 49 to 71) were included in the study. 3 POAG patients were excluded from the study, as manual adjustments of B-scan retinal segmentation were necessary.

Mean refractive error was -1.70 ± 2.31 diopters, ranging from -2.50D to +1.00D.

Both intraocular pressure (mean value 15.3 ± 1.2 mmHg) and central corneal thickness (mean value 557 ± 8 micron) were in the normal range.

Furthermore, the above parameters did not differ significantly between groups (p=0.543, and 0.413, respectively).

Thickness measurements of the different retinal layers provided by the new segmentation algorithm of the Spectralis SD-OCT "Posterior Pole" scans showed significant thinning of the total retinal, RNFL and GCL thickness in patients with early glaucoma when compared to controls, as demonstrated by the ANOVA test (p<0.0001). These results are presented in Table 1; graphs in Figures 2 and 3 show the statistically significant differences in the thickness of GCL and RNFL between the two groups. Figure 4 shows a comparison between a Posterior Pole GCL thickness map of a glaucoma patient and of a healthy subject, as obtained using the inbuilt Spectralis mapping software.

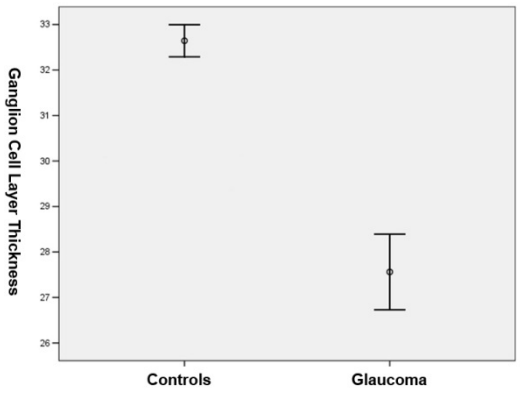

Figure 2: Graph of ANOVA results: Posterior Pole GCL thickness values in patients with glaucoma compared to controls.

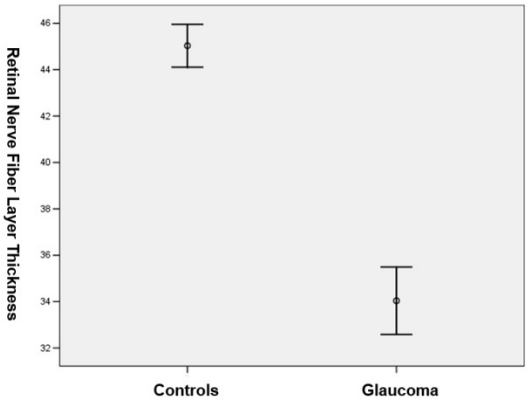

Figure 3: Graph of ANOVA results: Posterior Pole RNFL thickness values in patients with glaucoma compared to controls.

			ANOVA test		
Group	N*	Retina** (mean ± SD)	GCL** (mean ± SD)	RNFL** (mean ± SD)#	P§
Glaucoma	37	274,8 ± 15,0	27,6 ± 4,4	34,0 ± 7,7	<0.0001
Controls	40	294,13 ± 9,0	32,6 ± ,9	45,0 ± 5,1	<0.0001

*N: number of sample subjects **Retina: total retinal thickness; RNFL: retinal nerve fiber layer; GCL: ganglion cell layer #mean ± SD: mean value ± Standard deviation §p: p value

Table 1: Spectralis SD-OCT retinal posterior pole thickness values of Retina, Ganglion Cell Layer and Retinal Nerve Fiber Layer in patients with glaucoma compared to controls.

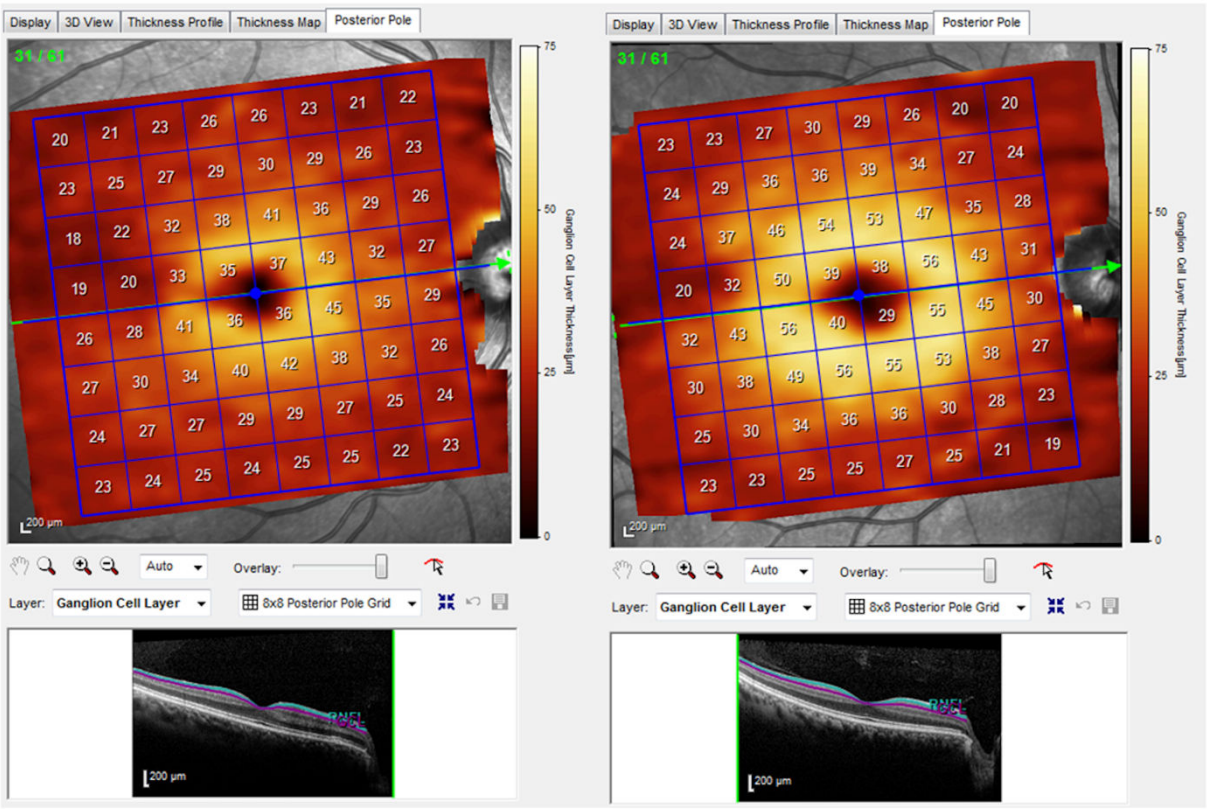

Figure 4: Comparison between Ganglion Cell Layer thickness map of a glaucoma patient (left) and of a healthy subject (right) as obtained using the inbuilt Spectralis mapping software.

Peripapillary RNFL thickness values differed significantly globally and in all sectors ($p<0.001$) between the two groups.

Pearson's correlation coefficient analysis showed that Posterior Pole RNFL thickness (ppRNFLt) correlated strongly with pRNFLt values ($r=0.863$) in glaucoma patients.

Signal strength did not differ between the glaucoma group and the healthy group ($p=0.762$).

The within-subject median CV% values and the between-subject median CV% values of all repeated measurements were found to be <5% for Total Retinal Thickness (Retina), GCL and Posterior Pole RNFL values, as shown in Tables 2 and 3, respectively.

Table 4 shows the between-subject median CV% values of each of the 64 retinal volumetric (total retinal thickness) units constituting the Spectralis Posterior Pole map. The values reproduce the topographical arrangement of the Spectralis Posterior Pole map with the exclusion of fovea-to-disc inclination; specifically T stands for temporal, N nasal, S superior and I inferior. Values in bold characters indicate very high reproducibility of the SD-OCT repeated measurements, while values in black indicate high reproducibility.

CV%*	Median	Min.	Max.
Retina**			
Subject 1	0,59	0,00	2,29
Subject 2	0,25	0,00	0,51
Subject 3	0,77	0,18	0,76
Subject 4	0,75	0,17	2,73
Subject 5	0,80	0,17	0,88
Subject 6	0,52	0,00	0,93
Subject 7	0,54	0,17	0,48
Subject 8	0,73	0,17	0,79
RNFL**			
Subject 1	3,42	0,00	0,78
Subject 2	2,87	0,00	10,19
Subject 3	3,99	0,00	18,55
Subject 4	4,55	0,93	14,04
Subject 5	4,61	0,00	0,78
Subject 6	3,03	0,00	12,49
Subject 7	3,11	0,00	10,83
Subject 8	3,85	0,00	13,07
GCL**			
Subject 1	2,63	0,00	7,02
Subject 2	2,67	0,00	10,14
Subject 3	2,33	0,00	7,81
Subject 4	3,74	0,00	16,47
Subject 5	3,22	0,00	19,68
Subject 6	3,13	0,00	12,95
Subject 7	3,11	0,00	9,52
Subject 8	3,23	0,00	16,90
*CV% : Coefficient of Variation; **Retina: total retinal thickness; RNFL: retinal nerve fiber layer; GCL: ganglion cell layer			

Table 2: Within-subject Coefficient of Variation % for the different retinal layers: median, minimum and maximum values of Posterior Pole total retinal (Retina), Retinal Nerve Fiber Layer (RNFL) and Ganglion Cell Layer (GCL) thickness.

Layer*	CV%**: Median (min. max.)
Retina	0,7 (0,2 ; ,5)
RNFL	3,7 (,7 ; 10,4)
GCL	3,2 (,1 ; 9,6)

*Layer: Retina: total retinal thickness; RNFL: retinal nerve fiber layer; GCL: ganglion cell layer

**CV%:: Coefficient of Variation (median, min. ;max.)

Table 3: Between-subject Coefficient of Variation % for the different retinal layer thicknesses: median, minimum and maximum values.

N	**S**								**T**
	0,98	0,48	0,57	0,50	0,47	0,39	0,84	0,28	0,56	
	0,67	0,75	0,50	0,50	0,85	0,83	0,92	0,74	0,72	
	0,92	0,56	0,75	0,58	0,51	0,80	0,80	0,88	0,73	
	0,68	0,66	0,50	**0,12**	**0,35**	0,30	0,63	0,85	0,76	
	0,48	0,63	0,37	0,59	0,86	0,46	0,71	**0,24**	0,67	
	0,73	0,45	0,76	0,68	0,87	**0,10**	**0,03**	**0,02**	0,83	
	0,32	0,62	0,80	0,83	0,67	**0,02**	0,94	0,52	0,84	
	0,76	**0,00**	0,62	0,73	0,83	0,80	0,83	0,89	0,81	
	0,82	0,64	0,61	0,69	0,80	0,71	0,84	0,80	0,74	
	I								

Bold characters indicate a very high repeatability of the SD-OCT repeated measurements, while values in black indicate a high repeatability. T: Temporal; N: Nasal; S: Superior; I: Inferior

Table 4: Between-subject Coefficient of Variation %: median values of Posterior Pole total retinal thickness (Retina).

Discussion

The new segmentation algorithm of the Spectralis SD-OCT allowed us to demonstrate a significant reduction of Total Retina, GCL and RNFL thickness in the whole retinal posterior pole in a group of patients with early glaucoma when compared to controls ($p<0.000$, Figures 1 and 2).

There are several reasons to perform an accurate study of the central retina in these patients: one of which being that in early

coherence tomography (SD-OCT) macular scans. Br J Ophthalmol 96: 1420-1425.

9. Nassif N, Cense B, Park B, Pierce M, Yun S, et al. (2004) In vivo high-resolution video-rate spectral-domain optical coherence tomography of the human retina and optic nerve. Opt Express 12: 367-376.
10. Wojtkowski M, Bajraszewski T, GorczyÅ„ska I, Targowski P, Kowalczyk A, et al. (2004) Ophthalmic imaging by spectral optical coherence tomography. Am J Ophthalmol 138: 412-419.
11. Bagci AM, Shahidi M, Ansari R, Blair M, Blair NP, et al. (2008) Thickness profiles of retinal layers by optical coherence tomography image segmentation. Am J Ophthalmol 146: 679-687.
12. Brusini P (2006) Staging the severity of disease in glaucoma. Arch Ophthalmol 124: 1795-1796.
13. European Glaucoma Society (2014) Terminology and Guidelines for Glaucoma, (4th edn).
14. Menke MN, Dabov S, Knecht P, Sturm V (2009) Reproducibility of retinal thickness measurements in healthy subjects using spectralis optical coherence tomography. Am J Ophthalmol. 147:467-477.
15. Schuman JS, Pedut-Kloizman T, Hertzmark E, Hee MR, Wilkins JR, et al. (1996) Reproducibility of nerve fiber layer thickness measurements using optical coherence tomography. Ophthalmology 103: 1889-1898.
16. Zeimer R, Asrani S, Zou S, Quigley H, Jampel H (1998) Quantitative detection of glaucomatous damage at the posterior pole by retinal thickness mapping. A pilot study. Ophthalmology 105: 224-231.
17. Curcio CA, Allen KA (1990) Topography of ganglion cells in human retina. J Comp Neurol 300: 5-25.
18. Seong M, Sung KR, Choi EH, Kang SY, Cho JW, et al. (2010) Macular and peripapillary retinal nerve fiber layer measurements by spectral domain optical coherence tomography in normal-tension glaucoma. Invest Ophthalmol Vis Sci 51: 1446-1452.
19. Tan O, Chopra V, Lu AT, Schuman JS, Ishikawa H, et al. (2009) Detection of macular ganglion cell loss in glaucoma by Fourier-domain optical coherence tomography. Ophthalmology 116: 2305-2314.
20. Garas A, Vargha P, Holló G (2011) Diagnostic accuracy of nerve fibre layer, macular thickness and optic disc measurements made with the RTVue-100 optical coherence tomograph to detect glaucoma. Eye (Lond) 25: 57-65.
21. Kim NR, Lee ES, Seong GJ, Kang SY, Kim JH, et al. (2011) Comparing the ganglion cell complex and retinal nerve fibre layer measurements by Fourier domain OCT to detect glaucoma in high myopia. Br J Ophthalmol 95: 1115-1121.
22. Schulze A, Lamparter J, Pfeiffer N, Berisha F, Schmidtmann I, et al. (2011) Diagnostic ability of retinal ganglion cell complex, retinal nerve fiber layer, and optic nerve head measurements by Fourier-domain optical coherence tomography. Graefes Arch Clin Exp Ophthalmol 249:1039-1045.
23. Rao HL, Babu JG, Addepalli UK, Senthil S, Garudadri CS (2012) Retinal nerve fiber layer and macular inner retina measurements by spectral domain optical coherence tomograph in Indian eyes with early glaucoma. Eye 26: 133-139.
24. Rao HL, Zangwill LM, Weinreb RN, Sample PA, Alencar LM, et al. (2010) Comparison of different spectral domain optical coherence tomography scanning areas for glaucoma diagnosis. Ophthalmology 117: 1692-1699.
25. Mori S, Hangai M, Sakamoto A, Yoshimura N (2010) Spectral-domain optical coherence tomography measurement of macular volume for diagnosing glaucoma. J Glaucoma 19: 528-534.
26. Mwanza JC, Oakley JD, Budenz DL, Chang RT, Knight OJ, et al. (2011) Macular ganglion cell-inner plexiform layer: automated detection and thickness reproducibility with spectral domain-optical coherence tomography in glaucoma. Invest Ophthalmol Vis Sci 52: 8323-8329.
27. Le PV, Zhang X, Francis BA, Varma R, Greenfield DS, et al. (2015) Advanced imaging for glaucoma study: design, baseline characteristics, and inter-site comparison. Am J Ophthalmol 159: 393-403.
28. Ctori I, Huntjens B (2015) Repeatability of Foveal Measurements Using Spectralis Optical Coherence Tomography Segmentation Software. PLoS One. 15: 10.
29. Harwerth RS, Quigley HA (2006) Visual field defects and retinal ganglion cell losses in patients with glaucoma. Arch Ophthalmol 124: 853-859.
30. Meyer zu Westrup V, Dietzel M, Pauleikhoff D, Hense HW (2014) The association of retinal structure and macular pigment distribution. Invest Ophthalmol Vis Sci 55: 1169-1175.
31. Zhang X, Loewen N, Tan O, Greenfield DS, Schuman JS, et al. (2015) Advanced Imaging for Glaucoma Study Group Predicting Development of Glaucomatous Visual Field Conversion Using Baseline Fourier-Domain Optical Coherence Tomography. Am J Ophthalmol S0002-9394.